The low-temperature photochromic response of bismuth germanium oxide

J. J. Martin, I. Foldvari, and C. A. Hunt
Department of Physics, Oklahoma State University, Stillwater, Oklahoma 74078-0444

Exposing the photorefractive bismuth germanium oxide (BGO) at low temperatures to 2.5–3.3 eV light produces photochromic absorption bands. In both undoped and Fe-doped material the absorption consists of overlapping bands at 1.5, 2.2, 2.7, and 3.1 eV. The 1.5- and 2.2-eV components are relatively weaker in Fe-doped BGO. In undoped BGO the photochromic bands anneal together above 200 K. Doping with iron adds an anneal stage in the 110–200 K range that matches the recovery of Fe^{3+}. Optical bleaching with 1.5-eV light was much less efficient than with visible band light. Thus, the 1.5-eV photochromic band may be an internal transition of the center responsible for the 2.2-eV band. In BGO:Al the aluminum electronically compensates the deep donor center responsible for the yellow coloration observed in undoped crystals. Photoexcitation at 9 K produces overlapping absorption bands at 1, 1.38, and 2.45 eV. All three bands have major anneal stage in the 80–100 K range. They also bleach out together when the sample is exposed to either infrared or visible range light. The $[AlO_4]^0$ center which causes the coloration observed in smoky quartz is a plausible model for the visible range photochromic center in BGO:Al.

I. INTRODUCTION

The sillenite structure compound bismuth germanium oxide, $Bi_{12}GeO_{20}$, BGO, is a photorefractive material of considerable current interest for optical signal processing applications.[1–10] Its properties are similar to those of the related compound bismuth silicon oxide, $Bi_{12}SiO_{20}$, BSO. In a number of insulating materials electrons (or holes) are trapped at impurities or other defects. When the crystal is exposed to light they are excited into the conduction (or valence) band where they migrate until they recombine at an empty shallower trap. If the light intensity pattern is nonuniform such as that formed by the crossed laser beams used in four-wave mixing, the distribution of retrapped charges is also nonuniform. This nonuniform charge distribution sets up a matching electric field pattern in the crystal. In noncentrosymmetric crystals such as BGO the electric field produces a corresponding pattern in the index of refraction through the electro-optic effect. This index change which was first found by Ashkin *et al.*,[11] in $LiNbO_3$ is known as the photorefractive effect. The lifetime of the grating depends upon the material, the temperature, and exposure to light.

Photoconductivity studies[12,13] suggest that the contribution by electrons to the photorefractive effect in BGO and BSO is at least an order of magnitude greater than that of holes; and both materials are usually regarded as *n* type. Early models of the photorefractive effect in these and other materials were based on the assumption that only one type of carrier and one trap were involved in the charge migration.[14,15] Mullen and Hellwarth[16] have determined the photorefractive parameters for *n*-type BSO. Recent studies suggest that both electron and hole migration, and multiple shallow and deep traps play a role in the photorefractive effect in BSO.[17–20] Attard and Brown[20] have found evidence for multiple shallow and deep traps in

BSO. Attard[21] has studied the shielding of the deep traps in BGO by photoexcited carriers and found that Valley's model[22] number 2 for simultaneous electron and hole transport applied.

The traps that take part in the photorefractive response in these oxide crystals are most likely impurities and other crystal defects. Unfortunately, the various grating experiments do not directly identify the traps involved. A number of point defect studies on undoped and doped BGO and BSO crystals have been carried out.[23–32] The yellow color of undoped BGO and BSO crystals is caused by a shoulder extending from about 2.5 eV to the absorption edge near 3.4 eV. The absorption shoulder is due to a deep electron donor;[12] and photorefractive gratings are usually written with a laser wavelength matching the shoulder. Colorless crystals can be grown by doping the melt with 1–5 mole % aluminum or gallium.[12,33–36] Aluminum in a germanium site will act as an acceptor and electronically compensate the donor. The nature of the donor is not understood. However, it appears to be related to deviations from stoichiometry. X-ray studies indicate that only 87% of the Ge (or Si) sites are occupied.[37] One possibility is bismuth occupying a germanium site.[35] The anti-site bismuth would be a donor. The work of Craig and Stephenson[38] supports this possibility. They found that the compound $Bi_{25}FeO_{40}$ which is perhaps better expressed as $Bi_{24}BiFeO_{40}$ has the same structure as BGO with Fe on one Ge site and Bi on the other in the bcc unit cell.

Thermally stimulated conductivity[12,35,36] and thermoluminescence[25,26,32,39–42] techniques have been used to study the electron and hole traps in BGO and BSO following optical excitation. At liquid nitrogen temperatures, optical excitation has been shown to induce absorption bands that are associated with some of the traps.[26,32] Since these bands decay as the sample is warmed to room temperature they can be used as an indicator of the stabil-

ity of some of the traps. We present results of a study of the production at 9 K and thermal stability of photochromic absorption bands in undoped, iron-doped and aluminum doped BGO.

II. EXPERIMENTAL PROCEDURE

Undoped and iron-doped BGO crystals were grown at Oklahoma State University for this study. The starting materials were Johnson–Mathey Grade-1 Bi_2O_3 and GeO_2. These were mixed in a stoichiometric ratio and then heat treated at 800 °C in a flowing oxygen atmosphere for 48 h. Iron doping was carried out by adding Fe_2O_3 with a corresponding reduction of GeO_2. Single crystals of BGO were grown in air using the Czochralski method on [100] seeds. The melt was contained in a platinum crucible. A pull rate of 2.5–3 mm/h and rotation rates of 30 to 86 rpm were used. The high rotation rate has been shown to suppress the core formation often found in BGO and BSO.[43] The highest rotation rates produced crystals with a square cross section. These crystals showed the yellow coloration typical of BGO and BSO.

A colorless aluminum doped (5 mole % Al_2O_3 in the melt) was provided by the Research Laboratory for Crystal Physics of the Hungarian Academy of Sciences, Budapest. A commercially grown undoped BGO optical sample was purchased from Crystal Technology for purposes of comparison.

Optical samples 1–1.5 mm thick with either (100) or (110) surfaces were cut from the crystals. The polished samples were mounted on the cold finger of a CTI closed-cycle cryogenic refrigerator so that they would be at a 45° angle to the sample beam of the Perkin–Elmer model 330 spectrophotometer used for the absorption measurements. The 45° mounting angle made it possible to expose the sample to the excitation light beam without removing the cold-head from the spectrophotometer. All optical scans were made with the sample held at 9–15 K.

The monochromatic source for excitation of the photochromic bands consisted of an Oriel 200-W Hg-Xe lamp and a Spex Minimate monochromator with 5-mm slits. The sample was held at 9–15 K while it was being photoexcited. The monochromator output was approximately 0.2 mW/cm². This source and several low-power lasers were also used for in situ bleaching experiments. The thermal stability of the photochromic bands were measured by carrying out isochronal anneals. After collecting a spectrum the temperature of the cold-finger was raised to the desired value and then returned to 9 K for the next data run.

III. RESULTS AND DISCUSSION

The absorption spectra taken at 10 K on the aluminum-doped BGO sample, the undoped BGO sample from Crystal Technology, and the iron-doped sample in the as-received condition are shown as solid lines in Fig. 1. The curves for each sample have been offset for clarity. The BGO:Fe sample was grown from a melt containing 2 mole
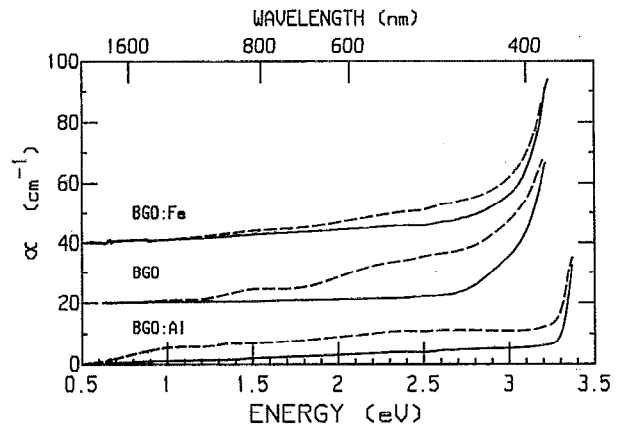

FIG. 1. Solid lines show the spectra taken at 10 K on the undoped BGO sample, the BGO:Fe, and the BGO:Al samples. The dashed lines show the additional photochromic absorption introduced by exposing the BGO and BGO:Fe samples to 3-eV light and the BGO:Al sample to 3.3-eV light.

% Fe. The shoulder on the absorption edge which causes the normal yellow coloration is missing in the colorless BGO:Al sample.

The dashed curves in Fig. 1 show the spectra taken on the three samples after they were exposed to intense (0.2 mW/cm²) monochromatic light for 1 h at 10 K. 3-eV light was used for the undoped and Fe-doped samples while 3.3-eV light was used for the Al-doped sample. The visible region photochromic absorption is similar to the liquid nitrogen temperature results reported by Jani and Halliburton[26] and by Foldvari et al.[32] The maximum photoinduced absorption is at approximately 2.6 eV for all of the samples.

Figure 2 shows the production of this additional absorption at 2.6 eV versus the energy of the incident photons for the BGO:Fe and BGO:Al samples. The curves have been corrected for the intensity variation of the monochromator output. The results for undoped BGO were the same as for BGO:Fe. The curve for the BGO:Fe sample shows that the photochromic bands are produced by excitation into the absorption shoulder on the band edge. The saturation observed above 2.8 eV is caused by the incident light beam not fully penetrating the sample. Lower energy pho-
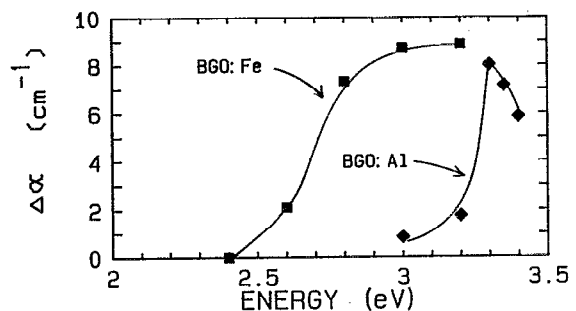

FIG. 2. Production of the photochromic absorption at 2.6 eV vs incident photon energy is shown for the BGO:Fe and BGO:Al samples. The results for the undoped BGO sample matched those of the BGO:Fe sample.
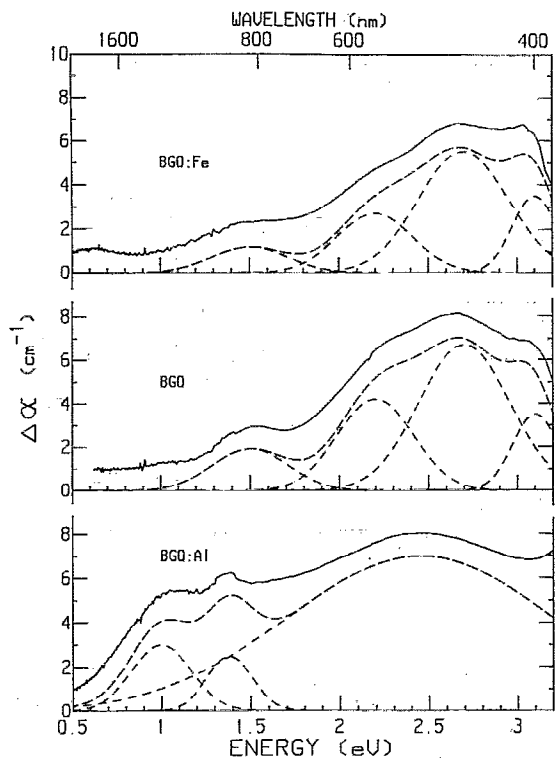
FIG. 3. Absorption spectra of the photochromic bands found by taking the difference between the curves in Fig. 1 are shown. The spectrum for the Al-doped sample extends further into the infrared than that of the others.

TABLE I. Estimated Gaussian band parameters.

Sample	Band (eV)	Half width (eV)	Strength (cm^{-1})
BGO	1.5	0.5	1.9
	2.2	0.5	4.2
	2.7	0.6	6.7
	3.1	0.7	3.5
BGO:Fe	1.5	0.5	1.2
	2.2	0.5	2.5
	2.7	0.6	5.5
	3.1	0.7	3.5
BGO:Al	1.0	0.4	3.0
	1.38	0.3	2.5
	2.45	1.75	7.0

tons tended to bleach the photochromic bands; this bleaching will be discussed below. The curve for the BGO:Al sample shows that a photon energy near 3.3 eV is needed to efficiently produce the additional absorption. The most efficient production occurs for photon energies matching the absorption shoulder in BGO and BGO:Fe and the band edge in BGO:Al.

Figure 3 shows the spectra of the photochromic absorption bands obtained by taking the difference between the dashed and solid curves shown in Fig. 1 for the three samples. The curves for the undoped and Fe-doped samples clearly show a band in the infrared at 1.5 eV and a stronger broad band in the visible region. This broad band may be made up of several overlapping bands. This possibility is illustrated by the dashed curves which show individual calculated Gaussian bands at 1.5, 2.2, 2.7, and 3.1 eV and their resulting composite possibility. Table I gives the parameters used to for these Gaussian bands. The 1.5- and 2.2-eV contributions were found to be consistently smaller in Fe-doped material than in undoped BGO. The 2.2-eV contribution also is approximately twice that of the 1.5-eV infrared band in both undoped and Fe-doped BGO. These results suggest that the infrared and 2.2-eV bands are due to the same center and that the 2.6-eV band is caused by a different center. The 3.1-eV component is more uncertain since above 3 eV the total absorption is so large that the uncertainties in the difference plots are large. The infrared and visible range components grew in at the same

rate and saturated after 30-min exposure.

The photochromic spectrum of BGO:Al is different than the spectra for undoped and Fe-doped material. As shown in Fig. 3 the spectrum extends further into the infrared with bands at or near 1 and 1.38 eV. The infrared bands are considerably stronger than the 1.5-eV band observed in the undoped and Fe-doped samples. There is also a featureless broad band centered at 2.45 eV. Again the infrared and visible range components grew at the same rate. The dashed curves show the calculated contribution from Gaussian bands at 1, 1.38, and 2.45 eV and their composite. In this case, the visible region band was treated as if it were a single band.

Isochronal anneal studies were carried out as follows. A background absorption spectrum was taken at 10 K; after the photochromic bands were "written" by exposing the sample to 3-eV light (3.3 eV for BGO:Al) their spectrum was then recorded. Then the sample was heated to the desired temperature and returned to 10 K where a new curve was recorded. This process was repeated for temperatures up to about 300 K. The contour plot in Fig. 4 shows the photochromic bands after subtracting the background curve as a function of anneal temperature for the undoped sample. While the 1.5-eV band shows a small decrease between 120 and 150 K, the major anneal stage starts at 220 K. Annealing to room temperature completely removes the bands. The major anneal starting at 220 K
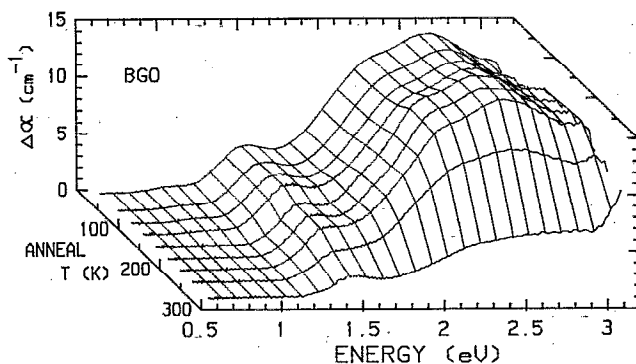

FIG. 4. This contour plot shows the thermal anneal of the photochromic bands in undoped BGO.
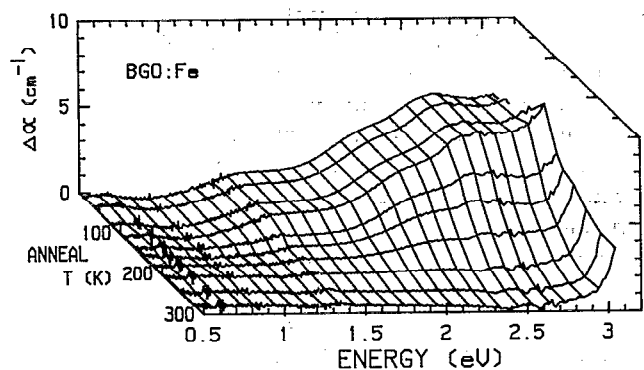
FIG. 5. This contour plot shows the thermal anneal of the BGO:Fe sample. Note that the major decay starts at 110 K in contrast to the decay in the undoped sample shown above.

matches the thermoluminescence signal (TSL), reported by Foldvari et al.[32] for undoped BGO.

Figure 5 shows the isochronal anneal results for the BGO:Fe sample. This sample was grown from a melt containing 2 mole % iron. The photochromic bands start to decay at about 110 K and have nearly disappeared by 200 K. This is the same temperature range for which Jani and Halliburton[26] reported the recovery of Fe^{3+}. In samples grown from melts with lower iron concentrations the decay levels off near 160 K; this is followed by the final decay above 220 K. While absorption bands that can be attributed to iron are not seen in these crystals iron is acting as a major trap and dominates the anneal characteristics of the BGO:Fe sample. Upturns above 3.0 eV are observed at the higher temperatures in most of our anneal results. These go out when the sample is held overnight at room temperature.

The isochronal anneal results for the photochromic bands in the Al-doped sample are shown in Fig. 6. The infrared bands (1 and 1.38 eV) anneal between 80 and 100 K; their decay is accompanied by the decay of a major portion of the visible range band. The remainder of the visible region band starts to decay near 175 K and is gone by 240 K. Foldvari et al.[32] have reported strong TSL peaks at 45, 65, and 115 K in a sample taken from the same
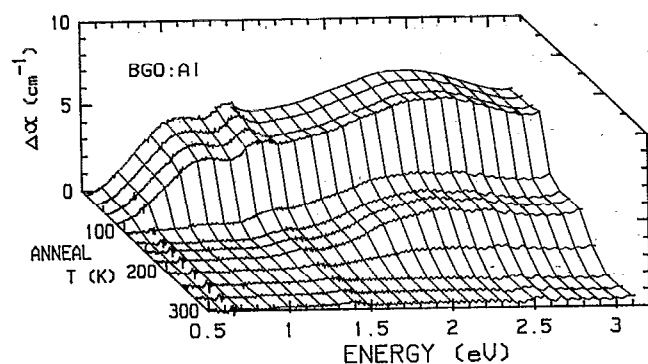

FIG. 6. Decay of the infrared photochromic bands in BGO:Al between 80 and 100 K is accompanied by the decay of a major portion of the visible band. The remainder of the bands decay between 175 and 230 K.
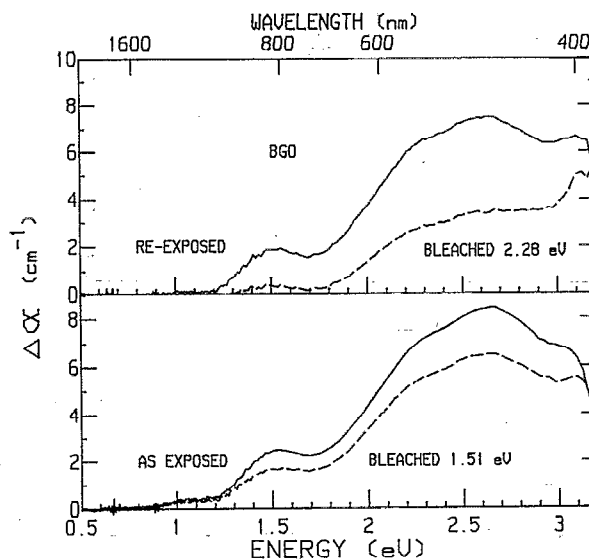

FIG. 7. Effects of bleaching with 2.28- and 1.51-eV laser light on the photochromic bands in undoped BGO is shown.

BGO:Al crystal used in these experiments. They had photoexcited their sample with 2.6-eV light. As shown in Fig. 2, 2.6-eV light is not able to efficiently produce these photochromic absorption bands and a direct comparison between the two experiments may not hold. After the 80–100 K decay stage the maximum of the visible band has shifted to a slightly lower energy suggesting that there may be other bands underlying the main band.

Several bleaching experiments were carried out using the Hg-Xe/monochromator source and several different low-power lasers. The upper solid curve in Fig. 7 shows the "as-written" photochromic bands in the undoped BGO sample. The dashed curve shows the result of then illuminating the sample (at 9 K) with a green (2.28 eV) 1-mW/cm^2 HeNe laser for 40 min. The 40-min bleach nearly removed the 1.5-eV band and significantly lowered the visible range band. It also produced an upturn above 3 eV similar to the anneal data. The lower set of curves shows that the bleaching caused by a 1.51-eV 3-mW/cm^2 diode laser is much less efficient. This result suggest that the 1.5-eV infrared band represents an internal transition rather than an excitation to the conduction band. Similar bleaching results were obtained for Fe-doped BGO samples.

The solid curve in Fig. 8 shows the "as-written" photochromic bands in the BGO:Al sample. Bleaching with a 0.84-eV 5-mW diode laser for 40 min lowered the bands as shown by the dashed curve. Faster bleaching occurred when the 1.51-eV diode laser or the 2.28-eV HeNe laser were used with the lower power green HeNe being the most efficient. A blue-green emission was visible to the eye when the 1.51-eV laser was used. This emission may have been masked when the green laser was used. The blue-green emission was not observed when the 0.84-eV laser was used. It was also not observed when the undoped samples were bleached with the 1.51-eV laser.
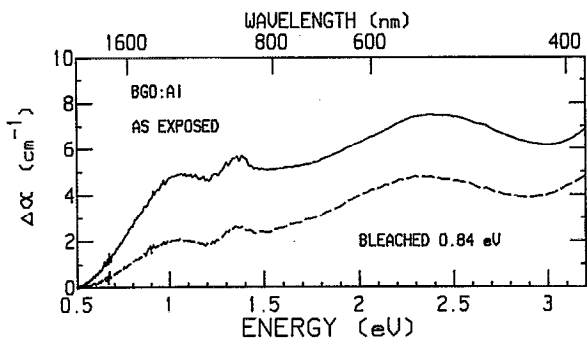
FIG. 8. Effects of bleaching with a 0.84-eV diode laser on the photochromic bands in BGO:Al are shown.

The nature of the defects acting as the electron donors and traps in BGO (and BSO) is not understood. The careful x-ray study carried out by Abrahams et al.[37] suggests that the Ge site is not fully occupied. Hou et al.[12] have suggested that Si vacancies act as the donor causing the absorption shoulder. BGO melts contain 12 times as much Bi as Ge and the possibility of an anti-site Bi should also be considered. This possibility was first suggested by Oberschmidt.[35] Craig and Stephenson[37] have shown that both Bi and Fe occupy the tetrahedrally bonded bcc Ge site in the compound $Bi_{24}BiFeO_{40}$. Bismuth in a Ge (or Si) site would act as a donor while iron would be an acceptor. Both would be paramagnetic. Fe^{3+} in the Ge or semi-insulating Si site has been confirmed using electron paramagnetic resonance (EPR) techniques.[26,41,42] Doping with iron removes some of the absorption shoulder but does not introduce additional bands. Iron does act as a trap and introduces an 110–200 K anneal stage in the photochromic bands.

Optical excitation into the absorption shoulder in undoped and Fe-doped BGO at low temperatures produces the bands shown in Fig. 3. The shape of the curves suggests bands at 1.5, 2.2, 2.7, and 3.1 eV. Bleaching into the 1.5-eV band is much less effective than bleaching at higher energies and, it is suppressed in the same ratio as the 2.2-eV band in Fe-doped crystals. Perhaps, the 1.3-eV emission reported by Lauer[39] for an excitation band peaking at 2.25 eV is a Stokes shifted emission corresponding to the 1.5-eV absorption reported here. Therefore, it seems plausible that the 1.5-eV band is an internal transition of the same center for which the 2.2-eV band is an excitation into the conduction band. It also seems likely that a different trap is responsible for the 2.7-eV band. Our bleaching results suggest that if both the 2.2- and 2.7-eV bands represent electron traps then the bands are excitations into the conduction band.

In aluminum-doped material, the Al occupies a Ge site and acts as an acceptor to compensate the deep donor. This compensation removes the absorption shoulder and, therefore, the yellow coloration of the crystal. At low temperatures, photochromic absorption bands are produced by using essentially band-edge light. The photochromic bands in BGO:Al are made up of relatively strong infrared bands at

1 and 1.38 eV and a broad, featureless visible band at 2.45 eV. The bands observed in the undoped crystals may be hidden under these bands. The bands decayed together when bleached with either infrared or visible light and the major portion decayed together at the 80–100 K anneal stage. A plausible model is that Al acts as a compensating acceptor with its available state filled by the electron from the donor. Band-gap light would excite the electron into the conduction band where it would drift until trapped and leave behind a hole trapped at the aluminum. This center is well known in quartz and is designated $[AlO_4]^0$ using Weil's notation; the hole is trapped on an nonbonding oxygen p orbital.[44] In quartz, the $[AlO_4]^0$ center has an associated broad absorption band that peaks near 2.5 eV.[45,46] One might speculate that the broad photochromic 2.45-eV band in BGO:Al is also due to the $[AlO_4]^0$ center. The $[AlO_4]^0$ EPR spectrum in BGO does not seem to have been reported. The band shows a very sharp anneal stage that starts at liquid nitrogen temperatures; consequently, lower temperatures need to be used to reliably produce the band. If the broad visible range band is the $[AlO_4]^0$ center then the infrared bands may represent the electron traps. This last assumption seems to be consistent with the bleaching and the annealing results.

IV. SUMMARY

At 9-K excitation into the absorption shoulder in the 2.5–3.3 eV range produces photochromic absorption bands in both undoped and Fe-doped BGO. These bands appear to consist of overlapping bands at 1.5, 2.2, 2.7, and 3.1 eV. The 1.5-eV infrared band is always weaker than the others and seems to track with the 2.2-eV band. Both the 1.5- and 2.2-eV bands are relatively weaker in BGO:Fe. In undoped BGO they anneal at temperatures above 200 K. Doping with iron adds an anneal stage in the 110–200 K range. 1.5-eV light bleached the bands much less efficiently than visible band light. The 1.5-eV band appears to be an internal transition of the center responsible for the 2.2-eV band. In BGO:Al the aluminum electronically compensates the deep donor causing the absorption shoulder in undoped crystals. At 9-K photoexcitation produces overlapping absorption bands at 1, 1.38, and 2.45 eV. These bands anneal together between 80 and 100 K. They also bleach out together when bleached by either infrared or visible light. The visible range photochromic band in aluminum doped material may be due to the $[AlO_4]^0$ center.

ACKNOWLEDGMENTS

[1] J. A. Neff, Opt. Eng. 26, 2 (1987).
[2] P. Gunther, Phys. Rep. 93, 199 (1982).
[3] J. P. Huignard, H. Railbenbach, Ph. Refregier, and L. Solymar, Opt. Eng. 17, 471 (1978).
[4] J. P. Huignard and F. Micheron, Appl. Phys. Lett. 29, 591 (1976).

[5] J. P. Huignard, J. P. Herriau, and T. Valentin, Appl. Opt. **16**, 2796 (1977).

[6] S. McCahon, J. Kim, and A. R. Tanguay, J. Opt. Soc. Am. A **1**, 1314 (1984).

[7] J. O. White and A. Yariv, Appl. Phys. Lett. **37**, 5 (1980).

[8] A. Marakchi, R. V. Johnson, and A. R. Tanguay, J. Opt. Soc. Am. B **3**, 321 (1986).

[9] C. L. Woods, C. L. Matson, and M. M. Salour, Appl. Phys. A **40**, 177 (1986).

[10] P. V. Lenzo, E. G. Spencer, and A. A. Ballman, Phys. Rev. Lett. **19**, 641 (1967).

[11] A. Ashkin, G. D. Boyd, J. M. Dziedzic, R. G. Smith, A. A. Ballman, H. J. Levinstein, and K. Nassau, Appl. Phys. Lett. **9**, 72 (1966).

[12] S. L. Hou, R. B. Lauer, and R. E. Aldrich, J. Appl. Phys. **44**, 2652 (1973).

[13] B. Kh. Kostyuk, A. Yu. Kudzin, and G. Kh. Sokloauskic, Sov. Phys. Solid State **22**, 1529 (1980).

[14] N. V. Kukhtarev, Sov. Tech. Phys. Lett. **2**, 438 (1976).

[15] N. V. Kukhtarev, V. B. Markov, S. G. Odulov, M. S. Soskin, and V. L. Vinestkii, Ferroelectrics **22**, 949 (1979).

[16] R. A. Mullen and R. W. Hellwarth, J. Appl. Phys. **58**, 40 (1985).

[17] F. P. Strokhendl and R. W. Hellwarth, J. Appl. Phys. **62**, 2450 (1987).

[18] F. P. Strokhendl, J. Appl. Phys. **65**, 3773 (1989).

[19] L. Arizmendi and R. C. Powell, J. Appl. Phys. **62**, 896 (1987).

[20] A. E. Attard and T. X. Brown, Appl. Opt. **25**, 3253 (1986).

[21] A. E. Attard, Appl. Opt. **27**, 232 (1988).

[22] G. C. Valley, J. Appl. Phys. **54**, 3363 (1986).

[23] D. B. Senulene, E. G. Babonas, E. I. Leonov, I. Muminov, and V. M. Orlov, Sov. Phys. Solid State **26**, 780 (1984).

[24] J. A. Baquedano, F. J. Lopez, and J. M. Cabrera, Solid State Commun. **72**, 233 (1989).

[25] A. P. Eliseev, V. A. Nadolinnyi, and V. A. Gusev, J. Struct. Chem. **23**, 484 (1982).

[26] M. G. Jani and L. E. Halliburton, J. Appl. Phys. **64**, 2022 (1988).

[27] L. B. Kuleva, E. I. Leonov, and V. M. Orlov, Sov. Phys. Solid State **29**, 1240 (1987).

[28] N. Benjellou, M. Tapiero, J. P. Zielinger, J. C. Launay, and F. Marsaud, J. Appl. Phys. **64**, 4013 (1988).

[29] L. B. Kuleva, E. I. Leonov, and V. M. Orlov, Sov. Phys. Solid State **30**, 536 (1988).

[30] T. V. Panchenko and N. A. Tryseeva, Ukr. Fiz. Zh. **34**, 1495 (1989).

[31] S. Denagbe, M. Martinaud, M. Schrorver, F. Marsand, J. C. Launay, and P. Hagenmuller, J. Phys. Chem. Solids **51**, 171 (1990).

[32] I. Foldvari, L. E. Halliburton, G. J. Edwards, and L. Otsi, Solid State Commun. **77**, 181 (1991).

[33] W. Rehwald, K. Frick, G. K. Lang, and E. Meier, J. Appl. Phys. **47**, 1292 (1976).

[34] B. C. Grabmayer and R. Oberschmidt, Phys. Status Solidi (a) **96**, 199 (1986).

[35] B. C. Grabmayer, Phys. Status Solidi (a) **89**, 263 (1985).

[36] T. V. Panchenko, A. Yu. Kudzin, and V. Kh. Kastyuk, Neorg. Mater. **19**, 1031 (1983).

[37] S. C. Abrahams, J. L. Berstein, and C. Svensson, J. Chem. Phys. **71**, 788 (1979).

[38] D. C. Craig and N. C. Stephenson, J. Solid State Chem. **15**, 1 (1975).

[39] R. B. Lauer, J. Appl. Phys. **42**, 2147 (1971).

[40] I. S. Zakharov, P. A. Petukhov, K. M. Kickulkin, A. V. Parlov, V. M. Sorikov, Ei. I. Leonov, Yu. F. Kargin, and A. D. Bondarev, Inorg. Mater. **22**, 379 (1986).

[41] H. J. von Bardelben, J. Phys. D **16**, 29 (1983).

[42] W. Wardzinski, M. Baran, and M. Szymczak, Physica **11B**, 47 (1981).

[43] P. J. Picone, J. Crystal Growth **87**, 421 (1988).

[44] J. A. Weil, Phys. Chem. Minerals **10**, 149 (1984).

[45] K. Nassau and B. E. Prescott, Phys. Status Solidi (a) **29**, 659 (1975).

[46] N. Koumvaklis, J. Appl. Phys. **51**, 5528 (1980).